Quercetin attenuates the symptoms of osteoarthritis *in vitro* and *in vivo* by suppressing ferroptosis via activation of AMPK/Nrf2/Gpx4 signaling

SHIYU DONG, XIAOLIANG LI, GENRONG XU, LIMING CHEN and JIYANG ZHAO

Department of Orthopedics, Beijing University of Chinese Medicine Third Affiliated Hospital, Beijing 100029, P.R. China

Received May 22, 2024; Accepted September 19, 2024

DOI: 10.3892/mmr.2024.13425

Abstract. Osteoarthritis (OA) is a common joint disorder involving the cartilage and other joint tissues. Quercetin (QCT) serves a protective role in the development of OA. However, to the best of our knowledge, the regulatory mechanisms of QCT in the progression of OA have not yet been fully elucidated. In order to mimic a model of OA *in vitro*, IL-1β was used to stimulate chondrocytes. Furthermore, an *in vivo* animal model of OA was induced by anterior cruciate ligament transection (ACLT). 5-Ethynyl-2'-deoxyuridine assays, TUNEL assays, ELISAs, western blotting and immunohistochemical assays were conducted to assess the chondroprotective properties of QCT in the development of OA. The results revealed that 100 μM QCT significantly promoted the proliferation, reduced the apoptosis and inflammation, and inhibited the extracellular matrix (ECM) degradation in IL-1β-stimulated chondrocytes. Additionally, QCT attenuated the IL-1β-induced ferroptosis of chondrocytes, as demonstrated by the reduced lipid reactive oxygen species and Fe^{2+} levels. Conversely, the inhibitory effects of QCT on the apoptosis and inflammatory responses were reversed by the activation of ferroptosis by erastin in IL-1β-stimulated chondrocytes. Furthermore, QCT significantly elevated the level of phosphorylated (p-)5' AMP-activated protein kinase (AMPK) and the levels of two negative regulators of ferroptosis [nuclear factor erythroid 2-related factor 2 (Nrf2) and glutathione peroxidase 4 (Gpx4)] in IL-1β-stimulated chondrocytes. The AMPK inhibitor compound C notably reversed the promoting effects of QCT on phosphorylated-AMPK, Nrf2 and Gpx4 expression in IL-1β-stimulated chondrocytes. Additionally, QCT markedly ameliorated the destruction and degradation of articular cartilage, and elevated the p-AMPK, Nrf2 and Gpx4 levels in the mouse model of ACLT-induced OA. Overall, the present study demonstrated that QCT inhibited the development of OA by suppressing ferroptosis via the activation of the AMPK/Nrf2/Gpx4 signaling pathway. These findings provide novel insights into the regulatory mechanisms of QCT for the treatment of patients with OA.

Correspondence to: Dr Jiyang Zhao, Department of Orthopedics, Beijing University of Chinese Medicine Third Affiliated Hospital, 51 Anwai Xiaoguan Street, Chaoyang, Beijing 100029, P.R. China
E-mail: jiyangzhao_88@163.com

Key words: osteoarthritis, quercetin, ferroptosis, 5' AMP-activated protein kinase, nuclear factor erythroid 2-related factor 2

Introduction

Osteoarthritis (OA) is a common type of arthritis, which is characterized by degenerative lesions of articular cartilage or other joint tissues (1-3). The incidence of OA is closely related to age (4). Prieto-Alhambra *et al* (4) reported that the incidence rate of knee and hip OA continues to increase with age. Turkiewicz *et al* (5) reported that the proportion of patients with OA aged ≥45 years may increase to ~30% by 2032. The increasing prevalence of OA will lead to a marked social and economic burden. Clinically, drug therapy, such as treatment with non-steroidal anti-inflammatory drugs and glucocorticoids, surgery, such as total hip arthroplasty, and physical therapy are commonly used methods for the treatment of OA (6-9). However, evidence has indicated that the long-term use of drugs used to treat OA is associated with a number of negative side effects, including gastrointestinal discomfort and liver function impairment (10,11). Thus, the development of promising novel treatment methods for OA is urgently required.

Traditional Chinese medicine (TCM) has been practiced in China for >5,000 years (12). TCM has been shown to exert a therapeutic effect on multiple diseases (13,14). Quercetin (QCT) is a bioactive compound that can be isolated from various TCM formulas, such as *Panax notoginseng* and *Ginkgo biloba* (15,16). QCT exhibits various pharmacological properties, including antioxidant, anti-inflammatory and anti-bacterial activities (17,18). Furthermore, QCT has been demonstrated to exert chondroprotective effects in murine models of OA (19,20). However, to the best of our knowledge, the mechanisms through which QCT attenuates the symptoms of OA remain largely unclear.

Ferroptosis is a type of iron-dependent cell death that is induced by iron accumulation and lipid peroxidation (21,22). Ferroptosis serves a crucial role in human diseases, including OA (23). Activation of ferroptosis is able to elevate the MMP13 levels and reduce the type II collagen (collagen II) levels in chondrocytes, suggesting that ferroptosis can contribute to the

progression of OA (23). However, whether QCT can attenuate the development of OA by affecting ferroptosis remains largely elusive.

In the present study, IL-1β-stimulated chondrocytes and a mouse model of anterior cruciate ligament transection (ACLT)-induced OA were established in order to explore the role of QCT in the treatment of OA disease.

Materials and methods

Cell culture. The human chondrocyte cell line (CHON-001; American Type Culture Collection) was cultured in DMEM (Gibco; Thermo Fisher Scientific, Inc.) containing 10% FBS (Gibco; Thermo Fisher Scientific, Inc.) with 1% Penicillin-Streptomycin Solution Hybri-Max™ (Sigma-Aldrich; Merck KGaA) at 37˚C in an incubator with 5% CO_2. To mimic an *in vitro* model of OA, CHON-001 cells were exposed to 10 ng/ml IL-1β (Novoprotein Scientific, Inc.) for 24 h at 37˚C (24). The 5' AMP-activated protein kinase (AMPK) inhibitor compound C, QCT and erastin were purchased from MedChemExpress, and the cells were treated with QCT (100 μM), QCT and erastin (5 μM) or QCT and compound C (5 μM) for 24 h at 37˚C, and then exposed to IL-1β for 24 h at 37˚C. Control cells were cultured in medium only.

Cell counting kit-8 (CCK-8) assay. CHON-001 cells were seeded ($5x10^4$ cells/well) in 96-well plates overnight. CHON-001 cells were treated with QCT (0, 25, 50, 100 or 200 μM) for 24 h at 37˚C. Subsequently, 10 μl CCK-8 reagent (Beyotime Institute of Biotechnology) was added to each well and the cells were incubated for a further 2 h at 37˚C. Subsequently, a microplate reader (MULTISKAN MK3; Thermo Fisher Scientific, Inc.) was used to detect the absorbance of each well at 450 nm. Similarly, CHON-001 cells were treated with QCT (50 or 100 μM) for 24 h at 37˚C, and then exposed to 10 ng/ml IL-1β for 24 h at 37˚C. The cell viability was detected with the CCK-8 assay as well. In addition, CHON-001 cells were treated with erastin (0, 1, 2, 5 or 10 μM) for 24 h at 37˚C and the cell viability was detected using a CCK-8 assay.

5-Ethynyl-2'-deoxyuridine (EdU) staining assay. Cell proliferation was detected using an EdU detection kit (Wuhan Servicebio Technology Co., Ltd.). The cells were fixed in 4% paraformaldehyde (Wuhan Servicebio Technology Co., Ltd.) for 2 h at room temperature and then stained with EdU Apollo567 solution for 1 h at 37˚C in the dark, followed by staining with 0.1 μg/ml DAPI (Wuhan Servicebio Technology Co., Ltd.) for 15 min at room temperature. Finally, the EdU-positive cells were observed using a fluorescence microscope (Eclipse Ci-L; Nikon Corporation). A total of three random fields were selected and the EdU-positive cells were counted manually.

TUNEL assay. A TUNEL detection kit (G1504; Wuhan Servicebio Technology Co., Ltd.) was applied to assess CHON-001 cell apoptosis. The cells were fixed in 4% paraformaldehyde for 2 h at room temperature and washed with PBS for 30 min. Subsequently, the cells were treated with 0.2% Triton X-100 for 2 min at room temperature. The cells were stained with the mixed solution (recombinant TdT enzyme:CF488-dUTP labeling mix:equilibration buffer, 1:5:50) for 1 h at 37˚C. The nuclei were stained with 0.1 μg/ml DAPI for 30 min in the dark at room temperature. Polyvinyl alcohol mounting medium with DABCO® (cat. no. 10981; Sigma-Aldrich; Merck KGaA) was used as the mounting medium. TUNEL-positive cells in three random fields were observed using a fluorescence microscope (Eclipse Ci-L; Nikon Corporation).

ELISA. Human IL-6 [cat. no. ELK1156; Elk (Wuhan) Biotechnology Co., Ltd.], TNF-α [cat. no. ELK1190; Elk (Wuhan) Biotechnology Co., Ltd.], glutathione (GSH; cat. no. A061-1; Nanjing Jiancheng Bioengineering Institute) and malondialdehyde (MDA; cat. no. A003-1; Nanjing Jiancheng Bioengineering Institute) detection kits were used to detect the IL-6, TNF-α, GSH and MDA levels in the supernatant of CHON-001 cells according to the manufacturers' instructions. Furthermore, the Fe^{2+} and lipid reactive oxygen species (ROS) levels in CHON-001 cells were detected using the Cell Ferrous Iron Colorimetric Assay kit (cat. no. E-BC-K881-M; Wuhan Elabscience Biotechnology Co., Ltd.) and BODIPY 581/591 C11 kit (cat. no. HY-D1301; MedChemExpress). All kits were used according to the manufacturers' instructions. The results were analyzed using a microplate reader (SMR16.1; Wuhan USCN Business Co., Ltd.).

Western blot analysis. Total protein was extracted from CHON-001 cells using RIPA buffer (Beyotime Institute of Biotechnology) and the protein concentration was measured using the BCA detection assay kit (ASPEN Biotechnology Co., Ltd.). Proteins (20 μg/lane) were resolved using 8% SDS-PAGE and transferred to PVDF membranes. After blocking with 5% non-fat milk for 1 h at room temperature, the membranes were incubated with primary antibodies against phosphorylated (p-)AMPK (cat. no. ab109402), AMPK (cat. no. ab32047), nuclear factor erythroid 2-related factor 2 (Nrf2; cat. no. ab31163), glutathione peroxidase 4 (Gpx4; cat. no. ab125066), Bcl-2 (cat. no. ab182858), cleaved caspase 3 (cat. no. ab214430), caspase 3 (cat. no. ab32351), aggrecan (cat. no. ab315486), collagen II (cat. no. ab34712), MMP13 (cat. no. ab219620), ADAM metallopeptidase with thrombospondin type 1 motif 5 (ADAMTS5; cat. no. ab41037) and β-actin (cat. no. ab8227) overnight at 4˚C. All primary antibodies were purchased from Abcam and the dilution factor was 1:1,000. The membranes were then probed with the secondary antibody (dilution, 1:5,000; cat. no. AS1107) for 2 h at room temperature. The secondary HRP-conjugated antibody was purchased from ASPEN Biotechnology Co., Ltd. Finally, the bands were visualized using ECL reagent (ASPEN Biotechnology Co., Ltd.). Densitometry was performed using ImageJ software (version 1.8.0; National Institutes of Health).

Animal experiments. C57BL/6 mice (8 weeks old; 18-22 g; female; n=24; 6 mice/group) were purchased from Beijing Vital River Laboratory Animal Technology Co., Ltd. All mice were housed with a 12-h light/dark cycle at 24˚C with 60% humidity, with *ad libitum* access to food and water. The experimental protocols were approved by the Ethics

Table I. Semi-quantitative scoring system.

Grade	Osteoarthritic damage
0	Normal
0.5	Loss of Safranin-O without structural changes
1	Small fibrillations without loss of cartilage
2	Vertical clefts down to the layer immediately below the superficial layer and some loss of surface lamina
3	Vertical clefts/erosion to the calcified cartilage extending to <25% of the articular surface
4	Vertical clefts/erosion to the calcified cartilage extending to 25-50% of the articular surface
5	Vertical clefts/erosion to the calcified cartilage extending to 51-75% of the articular surface
6	Vertical clefts/erosion to the calcified cartilage extending >75% of the articular surface

Committee of Beijing University of Chinese Medicine (approval no. BUCM-2023032701-2103; Beijing, China) and the animal experiments were performed according to the institutional guidelines. The animals were randomly divided into the following four groups: Sham, OA, OA + QCT 20 mg/kg and OA + QCT 40 mg/kg. The OA models were generated with ACLT surgery on the knee joints of the mice as previously described (25). The animals were treated with QCT (20 or 40 mg/kg) via gavage once per day for 4 weeks in the QCT treatment group. Mouse body weight loss >20% was regarded as a humane endpoint in the present study. The Osteoarthritis Research Society International (OARSI) score was determined based on the data of Safranin O/fast green staining to evaluate cartilage degradation (26). Briefly, a 0-6 subjective scoring system (0, 0.5, 1, 2, 3, 4, 5 and 6) was applied to all four quadrants of the joint: Medial femoral condyle, medial tibial plateau, lateral femoral condyle and lateral tibial plateau (Table I).

All animals were sacrificed using CO_2 at a displacement rate of 40% volume/min at 4 weeks following surgery, and the knee joints of each mouse were collected. The toe reaction and heartbeat of the mouse were checked to confirm animal death. The pathological changes of articular tissues were observed using H&E staining. Briefly, the samples were fixed in 4% paraformaldehyde for 24 h at room temperature and then embedded in paraffin. Subsequently, the specimens (4 μm thick) were placed in distilled water and then stained with hematoxylin for 15 min at room temperature. The sections were then rehydrated in alcohol at concentrations of 90 and 70% for 15 min each. Next, the sections were incubated with eosin staining solution for 10 min at room temperature. Afterwards, the samples were dehydrated with 100% alcohol and placed in in an incubator for drying. Images were captured using a light microscope (CS31; Olympus Corporation).

Safranin O/fast green staining assay. A modified Saffron-O and Fast Green Stain kit (cat. no. G1371; Beijing Solarbio Science & Technology Co., Ltd.) was used to evaluate the proteoglycan contents in the articular tissues. The samples were fixed in 4% paraformaldehyde for 24 h at room temperature and then embedded in paraffin. Paraffin sections of tissue were obtained from the embedded samples. The 4-μm paraffin sections were heated at 60˚C for 1 h, dewaxed twice in xylene solutions for 15 min each and rehydrated in a descending alcohol series. Subsequently, the articular tissue sections were stained with Weigert dye (Wuhan Servicebio Technology Co., Ltd.) for 5 min at room temperature. The sections were first stained with fast green solution for 5 min at room temperature and then stained with safranin O solution for 5 min at room temperature. Images were captured using a light microscope (CS31; Olympus Corporation).

Immunohistochemistry (IHC). The samples were fixed in 4% paraformaldehyde for 24 h at room temperature and then embedded in paraffin. Paraffin sections of tissue (4-μm) were obtained from the embedded samples and heated in a 60˚C oven. Subsequently, samples were deparaffinized, rehydrated in a descending alcohol series and boiled in 0.01 mol/l sodium citrate buffer (pH 6.0) in a microwave oven for 10 min for antigen retrieval. Next, samples were blocked with 0.3% hydrogen peroxide for 15 min at room temperature, and washed with distilled water. The sections were blocked for 30 min using 10% normal goat serum (Thermo Fisher Scientific, Inc.) at room temperature, and probed with primary antibodies specific for ADAMTS5 (1:100; cat. no. DF13268; Affinity Biosciences), MMP13 (1:300; cat. no. ab219620; Abcam), collagen II (1:200; cat. no. ab34712; Abcam) and aggrecan (1:150; cat. no. DF7561; Affinity Biosciences) overnight at 4˚C, and then incubated with a HRP-conjugated secondary antibody (1:200; cat. no. AS1107; ASPEN Biotechnology Co., Ltd.) for 30 min at 37˚C. The sections were stained with 3,3'-diaminodbenzidine solution (Wuhan Servicebio Technology Co., Ltd.). Subsequently, images were captured using a light microscope (CS31; Olympus Corporation). ImageJ software (version 1.8.0; National Institutes of Health) was used for analysis.

Statistical analysis. Data are presented as the mean ± SD. Multiple comparisons were conducted using one-way ANOVA with Tukey's post hoc test using GraphPad Prism 7 (Dotmatics). All experiments were repeated at least three times. $P<0.05$ was considered to indicate a statistically significant difference.

Results

QCT attenuates the IL-1β-induced apoptosis of chondrocytes. In order to determine the cytotoxic effects of QCT on chondrocytes, a CCK-8 assay was conducted. As

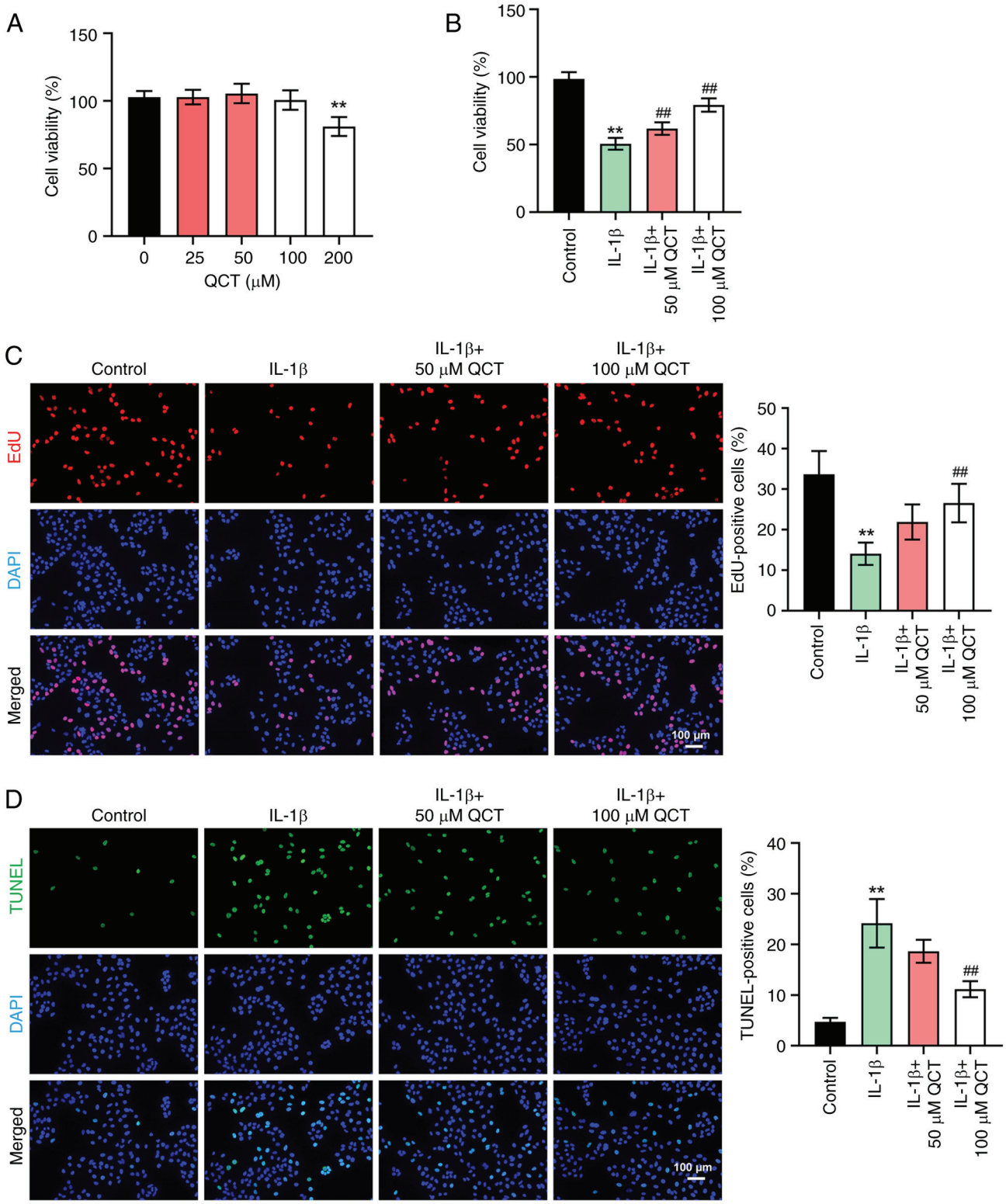

Figure 1. QCT attenuates IL-1β-induced apoptosis in chondrocytes. (A) CHON-001 cells were treated with QCT (0, 25, 50, 100 or 200 μM) for 24 h at 37˚C. Cell viability was detected using a CCK-8 assay. (B) CHON-001 cells were treated with QCT (50 or 100 μM) for 24 h at 37˚C, and then exposed to IL-1β for 24 h at 37˚C. Cell viability was detected using a CCK-8 assay. (C) Cell proliferation was evaluated using an EdU staining assay. Magnification, x200. Scale bar, 100 μm. (D) Cell apoptosis was assessed using a TUNEL assay. Magnification, x200. Scale bar, 100 μm. **P<0.01 vs. no QCT treatment or control group; $^{\#\#}$P<0.01 vs. IL-1β group. CCK-8, Cell Counting Kit-8; EdU, 5-ethynyl-2'-deoxyuridine; QCT, quercetin.

shown in Fig. 1A, 200 μM QCT significantly suppressed the viability of CHON-001 cells, while 50 or 100 μM QCT had a limited effect on CHON-001 cell viability. In addition, IL-1β markedly reduced the viability and proliferation, and triggered the apoptosis of CHON-001 cells; however, these changes were reversed by 100 μM QCT (Fig. 1B-D). Overall, QCT attenuated the IL-1β-induced injury of chondrocytes.

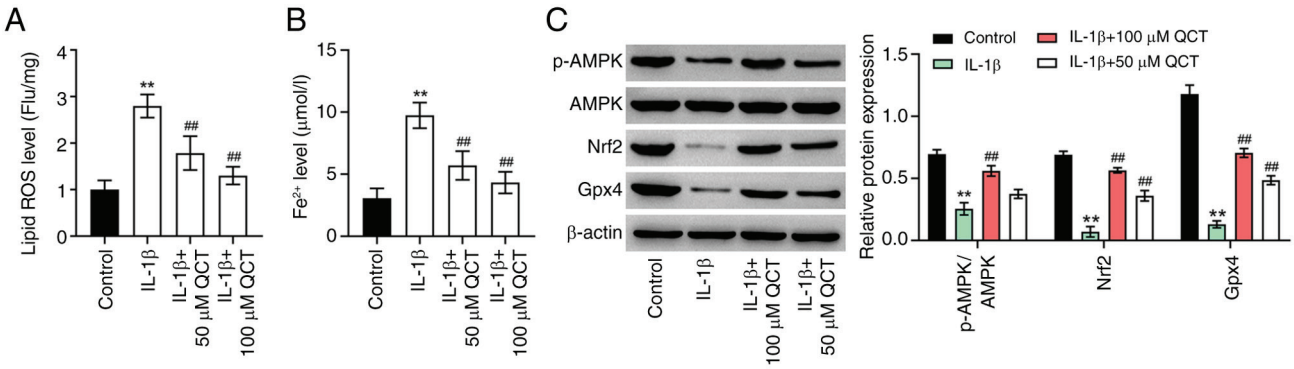

Figure 2. QCT inhibits IL-1β-induced ferroptosis in chondrocytes by activating AMPK/Nrf2/Gpx4 signaling. CHON-001 cells were treated with QCT (50 or 100 μM) for 24 h, and then exposed to IL-1β for 24 h. (A) Lipid ROS and (B) Fe^{2+} levels in CHON-001 cells were evaluated using ELISAs. (C) Western blotting was used to detect p-AMPK, AMPK, Nrf2 and Gpx4 levels in CHON-001 cells. The level of p-AMPK was normalized to that of AMPK. **P<0.01 vs. control group; $^{\#\#}$P<0.01 vs. IL-1β group. AMPK, 5' AMP-activated protein kinase; Gpx4, glutathione peroxidase 4; Nrf2, nuclear factor erythroid 2-related factor 2; p-, phosphorylated; QCT, quercetin; ROS, reactive oxygen species.

QCT inhibits the IL-1β-induced ferroptosis of chondrocytes by activating the AMPK/Nrf2/Gpx4 signaling pathway. To explore the effects of QCT on the ferroptosis of chondrocytes, lipid ROS and Fe^{2+} levels in CHON-001 cells were detected. IL-1β significantly enhanced lipid ROS and Fe^{2+} levels in CHON-001 cells; however, these effects were reversed by treatment with QCT (Fig. 2A and B). Additionally, treatment with 100 μM QCT significantly elevated the p-AMPK, Nrf2 and Gpx4 levels in CHON-001 cells exposed to IL-1β (Fig. 2C). In summary, QCT inhibited the IL-1β-induced ferroptosis of chondrocytes by activating the AMPK/Nrf2/Gpx4 signaling pathway.

QCT promotes the proliferation of IL-1β-stimulated chondrocytes by inhibiting ferroptosis. There is evidence to indicate that ferroptosis participates in the regulation of cell proliferation (27,28). Thus, in the present study, in order to explore whether QCT attenuated IL-1β-induced chondrocyte injury by modulating ferroptosis, erastin (a ferroptosis activator) was used. As shown in Fig. 3A, 5 μM erastin reduced CHON-001 cell viability to ~50%, with a significant difference compared with the 0 μM treatment group. Thus, 5 μM erastin was utilized in the subsequent experiments.

As shown in Fig. 3B-E, QCT markedly elevated the proliferation and prevented the apoptosis of IL-1β-stimulated CHON-001 cells; however, treatment with erastin reversed these effects. Additionally, QCT significantly elevated the Bcl-2 level and decreased the level of cleaved caspase 3 in the IL-1β-stimulated CHON-001 cells; however, the effects on these protein levels were reversed by erastin (Fig. 3F). Collectively, these results indicated that QCT promoted the proliferation of IL-1β-stimulated chondrocytes by inhibiting ferroptosis.

QCT attenuates extracellular matrix (ECM) degradation and inflammatory responses in IL-1β-stimulated chondrocytes by inhibiting ferroptosis. The present study then examined the effects of QCT on ECM degradation in IL-1β-stimulated chondrocytes. IL-1β significantly decreased the levels of ECM proteins (collagen II and aggrecan) and elevated the levels of ECM-degrading enzymes (MMP13 and ADAMTS5) in CHON-001 cells; however, the effects on these protein levels (except for ADAMTS5) were reversed by treatment with QCT (Fig. 4A and B). Conversely, treatment with erastin reversed the QCT-induced upregulation of collagen II and aggrecan and the downregulation of ADAMTS5 in IL-1β-stimulated CHON-001 cells (Fig. 4A and B). Additionally, QCT significantly reduced the IL-6, TNF-α, lipid ROS, Fe^{2+} and MDA levels, and increased the GSH level in CHON-001 cells exposed to IL-1β; however, erastin reversed these effects (Fig. 4C-H). Overall, QCT attenuated ECM degradation and inflammatory responses in IL-1β-stimulated chondrocytes by inhibiting ferroptosis.

QCT protects against IL-1β-induced ECM degradation in vitro by suppressing ferroptosis via the activation of the AMPK/Nrf2/Gpx4 signaling pathway. AMPK/Nrf2 signaling serves a crucial role in regulating ferroptosis (29). Therefore, the present study explored whether QCT could attenuate ferroptosis in chondrocytes by modulating AMPK/Nrf2 signaling. Treatment with QCT markedly elevated the p-AMPK, Nrf2 and Gpx4 levels in IL-1β-stimulated CHON-001 cells; however, these changes were reversed by treatment with compound C, an AMPK inhibitor (Fig. 5A). Furthermore, treatment with QCT markedly increased the aggrecan and collagen II levels, and reduced the ADAMTS5 level in IL-1β-stimulated CHON-001 cells, while compound C markedly reversed these effects (Fig. 5B). However, QCT had no effect on the MMP13 levels in IL-1β-stimulated CHON-001 cells (Fig. 5B). Collectively, QCT protected against IL-1β-induced ECM degradation *in vitro* by suppressing ferroptosis via the activation of the AMPK/Nrf2/Gpx4 signaling pathway.

QCT ameliorates OA in mice in vivo via activation of the AMPK/Nrf2/Gpx4 signaling pathway. Finally, to evaluate the therapeutic effects of QCT *in vivo*, a mouse model of OA was established. Disordered chondrocytes, damaged cartilage surface and proteoglycan loss in cartilage tissues were observed in the OA group; however, these effects were reversed by treatment with QCT, suggesting that QCT attenuated cartilage damage in mice with ACLT-induced OA

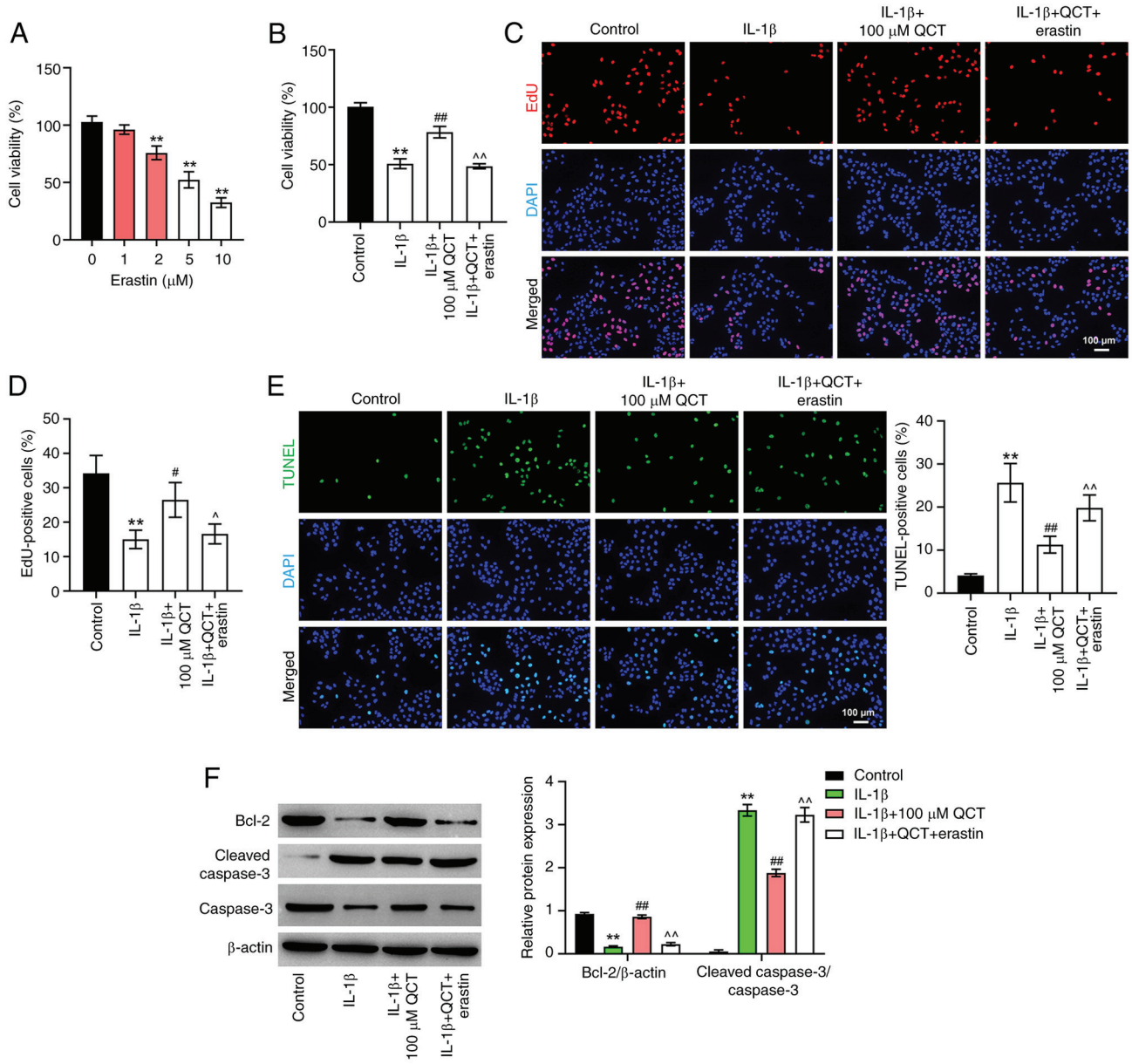

Figure 3. QCT promotes proliferation and inhibits apoptosis in IL-1β-treated chondrocytes by inhibiting ferroptosis. (A) CHON-001 cells were treated with erastin (0, 1, 2, 5 or 10 μM) for 24 h at 37˚C. Cell viability was detected using a CCK-8 assay. **P<0.01 vs. erastin (0 μM) group. (B) CHON-001 cells were treated with QCT (100 μM) or QCT and erastin (5 μM) for 24 h at 37˚C, and then exposed to IL-1β for 24 h at 37˚C. Cell viability was detected using a CCK-8 assay. (C) Cell proliferation was evaluated using an EdU staining assay. (D) EdU-positive cells were counted and quantified. Magnification, x200. Scale bar, 100 μm. (E) Cell apoptosis was assessed using a TUNEL assay. Magnification, x200. Scale bar, 100 μm. (F) Western blotting was used to detect Bcl-2, cleaved caspase 3 and caspase 3 levels in CHON-001 cells. **P<0.01 vs. control group; #P<0.05, ##P<0.01 vs. IL-1β group; ^P<0.05, ^^P<0.01 vs. IL-1β + QCT group. CCK-8, Cell Counting Kit-8; EdU, 5-ethynyl-2'-deoxyuridine; QCT, quercetin.

(Fig. 6A). Additionally, the results of IHC staining indicated that the aggrecan and collagen II levels were reduced, and the ADAMTS5 level was markedly elevated in the cartilage tissues of mice with OA, while these changes were reversed by treatment with 40 mg/kg QCT (Fig. 6A). However, QCT had no effect on the MMP13 level in the cartilage tissues of mice with OA (Fig. 6A). Furthermore, treatment with QCT significantly elevated the p-AMPK, Nrf2 and Gpx4 levels in cartilage tissues of mice with OA (Fig. 6B and C). The OARSI scores confirmed that QCT significantly attenuated the progression of OA (Fig. 6D). In summary, QCT ameliorated OA in mice *in vivo* via the activation of the AMPK/Nrf2/Gpx4 signaling pathway.

Discussion

It has been demonstrated that QCT exerts beneficial effects against multiple diseases, including diabetes mellitus, Alzheimer's and other neurodegenerative diseases and OA (30-32). Hu *et al* (19) found that QCT prevented the progression of OA in rats by attenuating cartilage degradation and suppressing chondrocyte apoptosis. Feng *et al* (33) indicated that QCT attenuated damage to rat chondrocytes by suppressing oxidative stress, endoplasmic reticulum stress and cell apoptosis. Qiu *et al* (20) found that QCT restored mitochondrial dysfunction and inhibited ECM degradation in rats with OA by activating AMPK/sirtuin 1 signaling, thereby

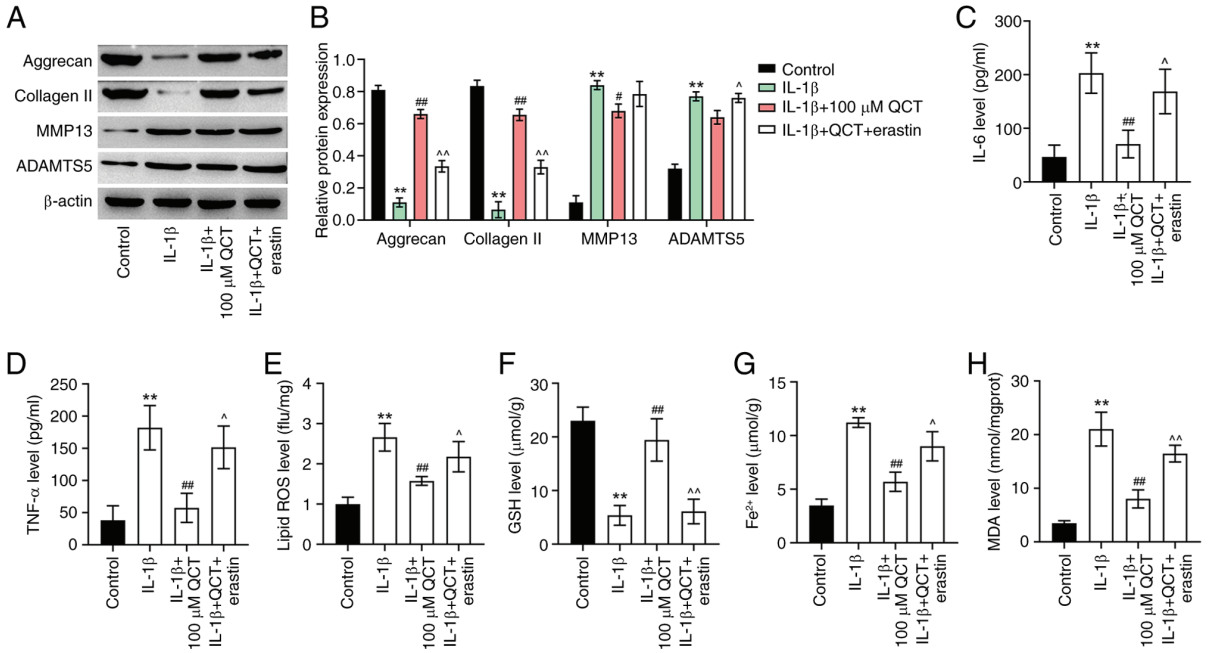

Figure 4. QCT attenuates extracellular matrix degradation and inflammatory responses in IL-1β-treated chondrocytes by inhibiting ferroptosis. (A) CHON-001 cells were treated with QCT (100 μM) or QCT and erastin (5 μM) for 24 h at 37˚C, and then exposed to IL-1β for 24 h. Western blotting was used to detect aggrecan, collagen II, MMP13 and ADAMTS5 levels in CHON-001 cells. (B) Relative expression levels of aggrecan, collagen II, MMP13 and ADAMTS5 were semi-quantified. CHON-001 cells were treated with QCT (100 μM) or QCT and erastin (5 μM) for 24 h at 37˚C, and then exposed to IL-1β for 24 h at 37˚C. (C) IL-6, (D) TNF-α, (E) lipid ROS, (F) GSH, (G) Fe^{2+} and (H) MDA levels in CHON-001 cells were evaluated using ELISAs. **P<0.01 vs. control group; $^{\#}$P<0.05, $^{\#\#}$P<0.01 vs. IL-1β group; $^{\wedge}$P<0.05, $^{\wedge\wedge}$P<0.01 vs. IL-1β + QCT group. ADAMTS5, ADAM metallopeptidase with thrombospondin type 1 motif 5; collagen II, type II collagen; GSH, glutathione; MDA, malondialdehyde; QCT, quercetin; ROS, reactive oxygen species.

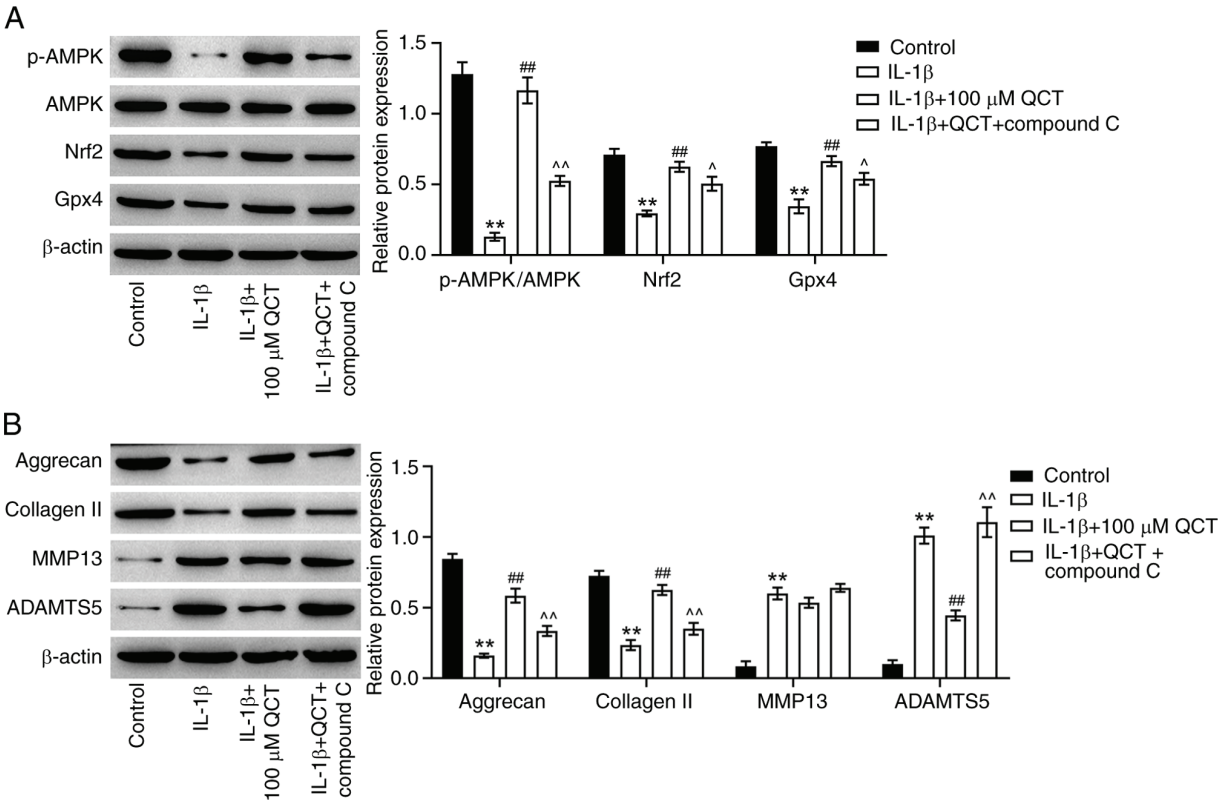

Figure 5. QCT protects against IL-1β-induced chondrocyte injury *in vitro* by suppressing ferroptosis via the activation of AMPK/Nrf2/Gpx4 signaling. CHON-001 cells were treated with QCT (100 μM) or QCT and compound C (5 μM) for 24 h at 37˚C, and then exposed to IL-1β for 24 h at 37˚C. (A) Western blotting was used to detect p-AMPK, AMPK, Nrf2 and Gpx4 levels in CHON-001 cells. The level of p-AMPK was normalized to that of AMPK. (B) Western blotting was used to detect aggrecan, collagen II, MMP13 and ADAMTS5 levels in CHON-001 cells. **P<0.01 vs. control group; $^{\#\#}$P<0.01 vs. IL-1β group; $^{\wedge}$P<0.05 $^{\wedge\wedge}$P<0.01 vs. IL-1β + QCT group. ADAMTS5, ADAM metallopeptidase with thrombospondin type 1 motif 5; AMPK, 5' AMP-activated protein kinase; collagen II, type II collagen; Gpx4, glutathione peroxidase 4; Nrf2, nuclear factor erythroid 2-related factor 2; p-, phosphorylated; QCT, quercetin.

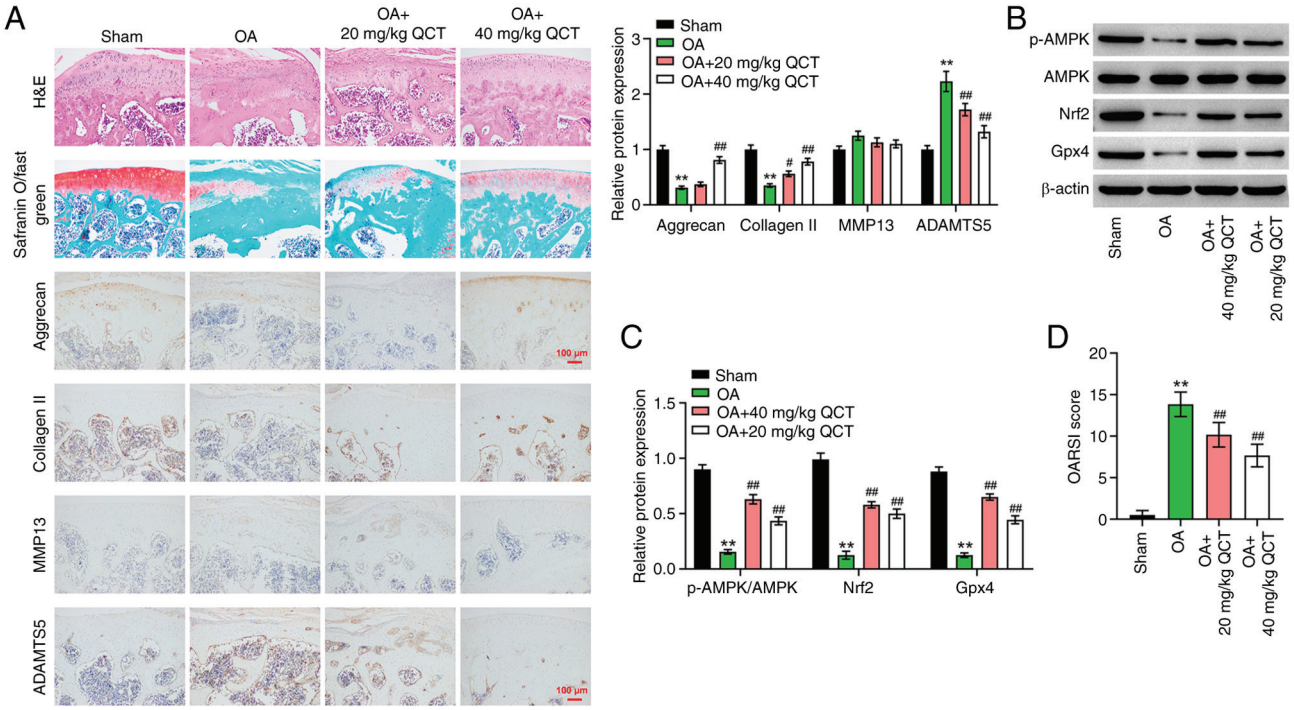

Figure 6. QCT ameliorates OA in mice *in vivo* via activation of AMPK/Nrf2/Gpx4 signaling. (A) Pathologic changes of mouse cartilage tissue were evaluated using H&E staining and safranin O/fast green assays. Immunohistochemistry was used to assess aggrecan, collagen II, MMP13 and ADAMTS5 levels in mouse cartilage tissues. Magnification, x200. Scale bar, 100 μm. (B) Western blotting was used to detect p-AMPK, AMPK, Nrf2 and Gpx4 levels in mouse cartilage tissues. (C) The level of p-AMPK was normalized to that of AMPK and the other proteins were normalized to β-actin. (D) OARSI score in each group. **P<0.01 vs. sham group; $^{\#}$P<0.05, $^{\#\#}$P<0.01 vs. OA group. ADAMTS5, ADAM metallopeptidase with thrombospondin type 1 motif 5; AMPK, 5' AMP-activated protein kinase; collagen II, type II collagen; Gpx4, glutathione peroxidase 4; Nrf2, nuclear factor erythroid 2-related factor 2; OA, osteoarthritis; OARSI, Osteoarthritis Research Society International; p-, phosphorylated; QCT, quercetin.

attenuating OA progression. These findings demonstrate the critical roles of QCT in the development of OA. The present study revealed a novel mechanism that underlies the chondroprotective effects of QCT in OA. In the present study, QCT markedly attenuated articular cartilage injury in mice with OA. Additionally, 100 μM QCT significantly enhanced the proliferation and reduced the apoptosis of IL-1β-stimulated chondrocytes. Furthermore, to the best of our knowledge, the present study was the first to demonstrate that QCT notably suppressed the ferroptosis of IL-1β-stimulated chondrocytes, as demonstrated by the reduced lipid ROS and Fe^{2+} levels. These results demonstrated that QCT attenuated the symptoms of OA by suppressing ferroptosis.

Chondrocyte ferroptosis has been found to aggravate the progression of OA (34). Ferroptosis is characterized by iron overload and the accumulation of lipid ROS (35). Furthermore, iron overload and lipid peroxidation are key pathological characteristics of OA (36,37). Iron overload is often observed in the tissues of elderly individuals, including knee joint tissues (38,39). Iron overload has been found to elevate the expression levels of the matrix-degrading enzymes MMP13 and ADAMTS5 in cartilage tissues (40,41). In the present study, lipid ROS production and the Fe^{2+} levels were markedly elevated in IL-1β-stimulated chondrocytes, suggesting that IL-1β induced ferroptosis in chondrocytes. However, treatment with QCT significantly reversed these effects. These data suggested that QCT possesses anti-ferroptosis properties in OA. Notably, the inhibition of chondrocyte ferroptosis has been found to attenuate the development of OA. For example, Zhou *et al* (42) found that curcumin exerted protective effects against erastin-induced ferroptosis in chondrocytes through the upregulation of Nrf2. He *et al* (43) indicated that biochanin A markedly attenuated articular cartilage injury in a mouse model of iron overload-associated OA by suppressing iron levels and activating Nrf2/Gpx4 signaling. Xu *et al* (44) found that tanshinone IIA was able to inhibit ECM degeneration in chondrocytes by inhibiting ferroptosis. The results of the present study demonstrated that treatment with QCT notably increased the aggrecan and collagen II levels in IL-1β-stimulated chondrocytes; however, the activation of ferroptosis evidently reversed these phenomena. Furthermore, the inhibitory effects of QCT on the apoptosis and inflammatory responses of IL-1β-stimulated chondrocytes were reversed by the activation of ferroptosis. Thereby, the present study indicated that QCT could prevent apoptosis, inflammation and ECM degradation in OA by suppressing ferroptosis.

AMPK can serve as an energy sensor that participates in a number of signal transduction pathways, including ferroptosis (45,46). The activation of AMPK signaling can inhibit ferroptotic cell death (46). Furthermore, the activation of AMPK signaling has been found to inhibit the development of OA in a mouse model of OA (47,48). There is evidence to indicate that AMPK can act as an activator of Nrf2 and Gpx4, two negative regulators of ferroptosis (49-51), suggesting that the activation of AMPK/Nrf2/Gpx4 signaling can suppress ferroptosis (52). Wan *et al* (53) revealed that baicalein was able to reduce chondrocyte ferroptosis by activating AMPK/Nrf2 signaling. Consistent with these previous findings, the present

study demonstrated that treatment with QCT elevated the p-AMPK, Nrf2 and Gpx4 levels in the cartilage tissues of mice with OA. Similarly, QCT significantly elevated the p-AMPK, Nrf2 and Gpx4 levels in IL-1β-stimulated chondrocytes; however, these changes were reversed by treatment with compound C, an AMPK inhibitor. Collectively, QCT suppressed ferroptosis *in vitro* and *in vivo* by activating the AMPK/Nrf2/Gpx4 signaling pathway.

However, whether QCT activation of AMPK/Nrf2/Gpx4 signaling was direct or indirect in the current study remains unclear. In addition, only one cell line was used in the present study, and the results should be validated using primary chondrocytes. Furthermore, the treatment duration in the animal experiment was relatively short (4 weeks), and it should be explored whether long-term effects could be observed. Although increasing evidence suggests that QCT protects against OA *in vitro* and *in vivo*, clinical testing of QCT is rare (54,55). Thus, it is difficult to suggest the advantages of QCT compared with other established anti-OA drugs such as oral non-steroidal anti-inflammatory drugs at present (6,7).

In conclusion, the findings of the present study demonstrated that QCT prevented the development of OA *in vitro* and *in vivo* by suppressing ferroptosis via the activation of AMPK/Nrf2/Gpx4 signaling. The findings illustrated that QCT could suppress chondrocyte ferroptosis via the activation of the AMPK/Nrf2/Gpx4 signaling pathway, providing novel insights into the regulatory mechanisms of QCT in OA. Additionally, these findings further support the potential use of QCT in the treatment of OA.

Acknowledgements

Not applicable.

Funding

No funding was received.

Availability of data and materials

The data generated in the present study may be requested from the corresponding author.

Authors' contributions

SD designed the overall study with contributions from XL. SD designed and carried out experiments, collected data and wrote the draft. XL, GX and LC carried out experiments and analyzed the data. SD, LC and JZ discussed and edited the paper. JZ supervised the study, designed experiments and cowrote the paper. SD and JZ confirm the authenticity of all the raw data. All authors have read and approved the final version of the manuscript.

Ethics approval and consent to participate

The protocols for animal care and use of laboratory animals were approved by the Ethics Committee of Beijing University of Chinese Medicine (approval no. BUCM-2023032701-2103; Beijing, China).

Patient consent for publication

Not applicable.

Competing interests

The authors declare that they have no competing interests.

References

1. Collins DP, Elsouri KN and Demory Beckler M: Osteoarthritis: Can we do better? Cureus 14: e31505, 2022.
2. Tavallaee G, Rockel JS, Lively S and Kapoor M: MicroRNAs in synovial pathology associated with osteoarthritis. Front Med (Lausanne) 7: 376, 2020.
3. Jiménez G, Cobo-Molinos J, Antich C and López-Ruiz E: Osteoarthritis: Trauma vs disease. Adv Exp Med Biol 1059: 63-83, 2018.
4. Prieto-Alhambra D, Judge A, Javaid MK, Cooper C, Diez-Perez A and Arden NK: Incidence and risk factors for clinically diagnosed knee, hip and hand osteoarthritis: Influences of age, gender and osteoarthritis affecting other joints. Ann Rheum Dis 73: 1659-1664, 2014.
5. Turkiewicz A, Petersson IF, Björk J, Hawker G, Dahlberg LE, Lohmander LS and Englund M: Current and future impact of osteoarthritis on health care: A population-based study with projections to year 2032. Osteoarthritis Cartilage 22: 1826-1832, 2014.
6. Ishijima M, Nakamura T, Shimizu K, Hayashi K, Kikuchi H, Soen S, Omori G, Yamashita T, Uchio Y, Chiba J, *et al*: Intra-articular hyaluronic acid injection versus oral non-steroidal anti-inflammatory drug for the treatment of knee osteoarthritis: A multi-center, randomized, open-label, non-inferiority trial. Arthritis Res Ther 16: R18, 2014.
7. Wang Q, Mol MF, Bos PK, Dorleijn DMJ, Vis M, Gussekloo J, Bindels PJE, Runhaar J and Bierma-Zeinstra SMA: Effect of intramuscular vs intra-articular glucocorticoid injection on pain among adults with knee osteoarthritis: The KIS randomized clinical trial. JAMA Netw Open 5: e224852, 2022.
8. Umpierres CS, Ribeiro TA, Marchisio ÂE, Galvão L, Borges ÍN, Macedo CA and Galia CR: Rehabilitation following total hip arthroplasty evaluation over short follow-up time: Randomized clinical trial. J Rehabil Res Dev 51: 1567-1578, 2014.
9. Safran-Norton CE, Sullivan JK, Irrgang JJ, Kerman HM, Bennell KL, Calabrese G, Dechaves L, Deluca B, Gil AB, Kale M, *et al*: A consensus-based process identifying physical therapy and exercise treatments for patients with degenerative meniscal tears and knee OA: The TeMPO physical therapy interventions and home exercise program. BMC Musculoskelet Disord 20: 514, 2019.
10. Ghouri A and Conaghan PG: Prospects for therapies in osteoarthritis. Calcif Tissue Int 109: 339-350, 2021.
11. Xie Z, Wang L, Chen J, Zheng Z, Srinual S, Guo A, Sun R and Hu M: Reduction of systemic exposure and side effects by intra-articular injection of anti-inflammatory agents for osteoarthritis: What is the safer strategy? J Drug Target 31: 596-611, 2023.
12. Siow YL, Gong Y, Au-Yeung KKW, Woo CWH, Choy PC and O K: Emerging issues in traditional Chinese medicine. Can J Physiol Pharmacol 83: 321-334, 2005.
13. Chan HHL and Ng T: Traditional Chinese medicine (TCM) and allergic diseases. Curr Allergy Asthma Rep 20: 67, 2020.
14. Sun H, Qu W, Chen G, Sun X, Zhang D and Shao S: Efficacy and safety of traditional Chinese patent medicine on carotid artery atherosclerosis in adults: A network meta-analysis protocol. Medicine (Baltimore) 100: e24406, 2021.
15. Ginkgo. In: Drugs and Lactation Database (LactMed®) [Internet]. National Institute of Child Health and Human Development, Bethesda, MD, 2006.
16. Li Y, Zhang N, Peng X, Ma W, Qin Y, Yao X, Huang C and Zhang X: Network pharmacology analysis and clinical verification of Jishe Qushi capsules in rheumatoid arthritis treatment. Medicine (Baltimore) 102: e34883, 2023.
17. Qi W, Qi W, Xiong D and Long M: Quercetin: Its antioxidant mechanism, antibacterial properties and potential application in prevention and control of toxipathy. Molecules 27: 6545, 2022.

18. Beken B, Serttas R, Yazicioglu M, Turkekul K and Erdogan S: Quercetin improves inflammation, oxidative stress, and impaired wound healing in atopic dermatitis model of human keratinocytes. Pediatr Allergy Immunol Pulmonol 33: 69-79, 2020.
19. Hu Y, Gui Z, Zhou Y, Xia L, Lin K and Xu Y: Quercetin alleviates rat osteoarthritis by inhibiting inflammation and apoptosis of chondrocytes, modulating synovial macrophages polarization to M2 macrophages. Free Radic Biol Med 145: 146-160, 2019.
20. Qiu L, Luo Y and Chen X: Quercetin attenuates mitochondrial dysfunction and biogenesis via upregulated AMPK/SIRT1 signaling pathway in OA rats. Biomed Pharmacother 103: 1585-1591, 2018.
21. Li J, Cao F, Yin HL, Huang ZJ, Lin ZT, Mao N, Sun B and Wang G: Ferroptosis: Past, present and future. Cell Death Dis 11: 88, 2020.
22. Chen X, Kang R, Kroemer G and Tang D: Ferroptosis in infection, inflammation, and immunity. J Exp Med 218: e20210518, 2021.
23. Miao Y, Chen Y, Xue F, Liu K, Zhu B, Gao J, Yin J, Zhang C and Li G: Contribution of ferroptosis and GPX4's dual functions to osteoarthritis progression. EBioMedicine 76: 103847, 2022.
24. Xiao P, Zhu X, Sun J, Zhang Y, Qiu W, Li J and Wu X: MicroRNA-613 alleviates IL-1β-induced injury in chondrogenic CHON-001 cells by targeting fibronectin 1. Am J Transl Res 12: 5308-5319, 2020.
25. Kamekura S, Hoshi K, Shimoaka T, Chung U, Chikuda H, Yamada T, Uchida M, Ogata N, Seichi A, Nakamura K and Kawaguchi H: Osteoarthritis development in novel experimental mouse models induced by knee joint instability. Osteoarthritis Cartilage 13: 632-641, 2005.
26. Glasson SS, Chambers MG, Van Den Berg WB and Little CB: The OARSI histopathology initiative-recommendations for histological assessments of osteoarthritis in the mouse. Osteoarthritis Cartilage 18 (Suppl 3): S17-S23, 2010.
27. Lin Z, Liu J, Kang R, Yang M and Tang D: Lipid metabolism in ferroptosis. Adv Biol (Weinh) 5: e2100396, 2021.
28. Zheng Q, Li P, Zhou X, Qiang Y, Fan J, Lin Y, Chen Y, Guo J, Wang F, Xue H, *et al*: Deficiency of the X-inactivation escaping gene KDM5C in clear cell renal cell carcinoma promotes tumorigenicity by reprogramming glycogen metabolism and inhibiting ferroptosis. Theranostics 11: 8674-8691, 2021.
29. Lu Q, Yang L, Xiao JJ, Liu Q, Ni L, Hu JW, Yu H, Wu X and Zhang BF: Empagliflozin attenuates the renal tubular ferroptosis in diabetic kidney disease through AMPK/NRF2 pathway. Free Radic Biol Med 195: 89-102, 2023.
30. Zu G, Sun K, Li L, Zu X, Han T and Huang H: Mechanism of quercetin therapeutic targets for Alzheimer disease and type 2 diabetes mellitus. Sci Rep 11: 22959, 2021.
31. Bayazid AB and Lim BO: Quercetin is an active agent in berries against neurodegenerative diseases progression through modulation of Nrf2/HO1. Nutrients 14: 5132, 2022.
32. Aleebrahim-Dehkordi E, Soveyzi F, Arian AS, Hamedanchi NF, Hasanpour-Dehkordi A and Rafieian-Kopaei M: Quercetin and its role in reducing the expression of pro-inflammatory cytokines in osteoarthritis. Antiinflamm Antiallergy Agents Med Chem 21: 153-165, 2023.
33. Feng K, Chen Z, Pengcheng L, Zhang S and Wang X: Quercetin attenuates oxidative stress-induced apoptosis via SIRT1/AMPK-mediated inhibition of ER stress in rat chondrocytes and prevents the progression of osteoarthritis in a rat model. J Cell Physiol 234: 18192-18205, 2019.
34. Zhou X, Zheng Y, Sun W, Zhang Z, Liu J, Yang W, Yuan W, Yi Y, Wang J and Liu J: D-mannose alleviates osteoarthritis progression by inhibiting chondrocyte ferroptosis in a HIF-2α-dependent manner. Cell Prolif 54: e13134, 2021.
35. Wu X, Li Y, Zhang S and Zhou X: Ferroptosis as a novel therapeutic target for cardiovascular disease. Theranostics 11: 3052-3059, 2021.
36. Zhang S, Xu J, Si H, Wu Y, Zhou S and Shen B: The role played by ferroptosis in osteoarthritis: Evidence based on iron dyshomeostasis and lipid peroxidation. Antioxidants (Basel) 11: 1668, 2022.
37. Dai T, Xue X, Huang J, Yang Z, Xu P, Wang M, Xu W, Feng Z, Zhu W, Xu Y, *et al*: SCP2 mediates the transport of lipid hydroperoxides to mitochondria in chondrocyte ferroptosis. Cell Death Discov 9: 234, 2023.
38. Burton LH, Radakovich LB, Marolf AJ and Santangelo KS: Systemic iron overload exacerbates osteoarthritis in the strain 13 guinea pig. Osteoarthritis Cartilage 28: 1265-1275, 2020.
39. Gozzelino R and Arosio P: Iron homeostasis in health and disease. Int J Mol Sci 17: 130, 2016.
40. Jing X, Du T, Li T, Yang X, Wang G, Liu X, Jiang Z and Cui X: The detrimental effect of iron on OA chondrocytes: Importance of pro-inflammatory cytokines induced iron influx and oxidative stress. J Cell Mol Med 25: 5671-5680, 2021.
41. Jing X, Lin J, Du T, Jiang Z, Li T, Wang G, Liu X, Cui X and Sun K: Iron overload is associated with accelerated progression of osteoarthritis: The role of DMT1 mediated iron homeostasis. Front Cell Dev Biol 8: 594509, 2021.
42. Zhou Y, Jia Z, Wang J, Huang S, Yang S, Xiao S, Xia D and Zhou Y: Curcumin reverses erastin-induced chondrocyte ferroptosis by upregulating Nrf2. Heliyon 9: e20163, 2023.
43. He Q, Yang J, Pan Z, Zhang G, Chen B, Li S, Xiao J, Tan F, Wang Z, Chen P and Wang H: Biochanin A protects against iron overload associated knee osteoarthritis via regulating iron levels and NRF2/System xc-/GPX4 axis. Biomed Pharmacother 157: 113915, 2023.
44. Xu J, Zhi X, Zhang Y and Ding R: Tanshinone IIA alleviates chondrocyte apoptosis and extracellular matrix degeneration by inhibiting ferroptosis. Open Life Sci 18: 20220666, 2023.
45. Ge Y, Zhou M, Chen C, Wu X and Wang X: Role of AMPK mediated pathways in autophagy and aging. Biochimie 195: 100-113, 2022.
46. Lee H, Zandkarimi F, Zhang Y, Meena JK, Kim J, Zhuang L, Tyagi S, Ma L, Westbrook TF, Steinberg GR, *et al*: Energy-stress-mediated AMPK activation inhibits ferroptosis. Nat Cell Biol 22: 225-234, 2020.
47. Li J, Zhang B, Liu WX, Lu K, Pan H, Wang T, Oh CD, Yi D, Huang J, Zhao L, *et al*: Metformin limits osteoarthritis development and progression through activation of AMPK signalling. Ann Rheum Dis 79: 635-645, 2020.
48. Jin Z, Chang B, Wei Y, Yang Y, Zhang H, Liu J, Piao L and Bai L: Curcumin exerts chondroprotective effects against osteoarthritis by promoting AMPK/PINK1/Parkin-mediated mitophagy. Biomed Pharmacother 151: 113092, 2022.
49. Ding X, Jian T, Li J, Lv H, Tong B, Li J, Meng X, Ren B and Chen J: Chicoric acid ameliorates nonalcoholic fatty liver disease via the AMPK/Nrf2/NFκB signaling pathway and restores gut microbiota in high-fat-diet-fed mice. Oxid Med Cell Longev 2020: 9734560, 2020.
50. Ge MH, Tian H, Mao L, Li DY, Lin JQ, Hu HS, Huang SC, Zhang CJ and Mei XF: Zinc attenuates ferroptosis and promotes functional recovery in contusion spinal cord injury by activating Nrf2/GPX4 defense pathway. CNS Neurosci Ther 27: 1023-1040, 2021 (Epub ahead of print).
51. Zhang Y, Wu Q, Liu J, Zhang Z, Ma X, Zhang Y, Zhu J, Thring RW, Wu M, Gao Y and Tong H: Sulforaphane alleviates high fat diet-induced insulin resistance via AMPK/Nrf2/GPx4 axis. Biomed Pharmacother 152: 113273, 2022.
52. Lu H, Xiao H, Dai M, Xue Y and Zhao R: Britanin relieves ferroptosis-mediated myocardial ischaemia/reperfusion damage by upregulating GPX4 through activation of AMPK/GSK3β/Nrf2 signalling. Pharm Biol 60: 38-45, 2022.
53. Wan Y, Shen K, Yu H and Fan W: Baicalein limits osteoarthritis development by inhibiting chondrocyte ferroptosis. Free Radic Biol Med 196: 108-120, 2023.
54. Samadi F, Kahrizi MS, Heydari F, Arefnezhad R, Roghani-Shahraki H, Mokhtari Ardekani A and Rezaei-Tazangi F: Quercetin and osteoarthritis: A mechanistic review on the present documents. Pharmacology 107: 464-471, 2022.
55. Yamaura K, Nelson AL, Nishimura H, Rutledge JC, Ravuri SK, Bahney C, Philippon MJ and Huard J: Therapeutic potential of senolytic agent quercetin in osteoarthritis: A systematic review and meta-analysis of preclinical studies. Ageing Res Rev 90: 101989, 2023.